Spatial heterogeneity in distance decay of using bike sharing: An empirical large-scale analysis in Shanghai

Kun Gao [a], Ying Yang [b],[*], Aoyong Li [c], Xiaobo Qu [a]

[a] *Department of Architecture and Civil Engineering, Chalmers University of Technology, Gothenburg SE-412 96, Sweden*
[b] *School of Behavioural and Health Sciences, Australian Catholic University, Strathfield, Australia*
[c] *Institute for Transport Planning and Systems (IVT), ETH Zürich, Zürich CH-8093, Switzerland*

A B S T R A C T

Distance decay is a vital aspect for modeling spatial interactions of human movements and an indispensable input for land use planning and travel demand prediction models. Although many studies have investigated the usage demand of bike-sharing systems in an area, research investigating the distance decay patterns of using dockless bike-sharing systems (DLBS) from a spatially heterogeneous perspective based on large-scale datasets is lacking. This study firstly utilizes massive transaction record data from DLBS in Shanghai of China and online map navigator Application Programming Interface to empirically estimate the distance decay patterns of using DLBS and reveal the spatial heterogeneity in distance decay of using DLBS across different urban contexts. Afterward, this study examines the mechanism of spatial heterogeneity in distance decay, leveraging multiple data resources including Point of Interest (POI) data, demographic data, and road network data. The associations among the distance decay of using DLBS with built environment factors are investigated by multiple linear regression. Results indicate that factors such as population density, land use entropy, branch road density, and metro station density are significantly related to larger distance decay of using DLBS, while factors such as commercial land use ratio, industrial land use ratio, and motorway density are significantly linked to smaller distance decay in Shanghai. Lastly, we further employ an adaptative geographically weighted regression to investigate the spatial divergences of the influences of built environment factors on distance decay. Results reveal notably distinct and even inverse influences of a built environment factor on the distance decay of using DLBS in different urban contexts. The findings provide insights into the distance decay patterns of using DLBS in different urban contexts and their interactions with the built environment, which can support accurate planning and management of sustainable DLBS as per specific urban characteristics.

1. Introduction

The bike-sharing system, as a relatively new alternative and environmentally friendly travel choice, has been increasingly prevalent in major metropolises around the world (Chen et al., 2020; Gao et al., 2021; Jin et al., 2015; Lazarus et al., 2020; Wang et al., 2021). The number of deployed bikes in worldwide bike-sharing systems is estimated to reach 23.2 million by the end of 2019 (Svegander, 2020). The bike-sharing systems appeared as the form of docked bike-sharing systems with fixed stations in the early stage and recently

evolved to be dockless bike-sharing systems (DLBS) with improved flexibility (Chen et al., 2020; Guo and He, 2020). DLBS is demonstrated to be beneficial for mitigating transport emissions, promoting multimodal transport connections, and improving public health (Barbour et al., 2019; Zhang and Mi, 2018). Nonetheless, the development of DLBS encounter appearing concerns. For instance, imbalances between supplies and demands in spatial and temporal dimensions have been a barrier for the takeup of DLBS (Wang et al., 2018; Pal and Zhang, 2017); unorderly parking and unsuited allocations of bicycles result in deuterogenic traffic issues (e.g., occupying pedestrian and driving lanes) and low utilization rates (Wang et al., 2020; Sun et al., 2019; Shui and Szeto, 2018).

To plan, design, and manage DLBS effectively and sustainably, one of the cores is to decipher the patterns of spatial interactions using DLBS. Spatial interactions in geography refer to the dynamic movement flows of human beings or goods in the spatial dimension (Fotheringham and O'Kelly, 1989). A crucial task of modeling the patterns of spatial interactions is to determine the distance decay (Zhu et al., 2020; Yang et al., 2019), which reflects the famous first law of geography "everything is related to everything else, but near things are more related than distant things" (Tobler, 1970). The distance decay denotes how the strengths of spatial interactions reduce with distance increasing. Insights into the law of distance decay are important for modeling and predicting the spatial distribution of travel demands, and deciphering the underlying relationships between the demands and geographical factors such as land use and transport infrastructure (Zhu et al., 2020; Yang et al., 2019). Additionally, the distance decay is also an indispensable component for evaluating the accessibility of using DLBS, and thus is an essential basis for planning initiatives and land use developments designed to promote DLBS (Yang et al., 2019; Arranz-López et al., 2019). Comparing to quite a few studies regarding usage amount or patterns of bike-sharing systems in an area (e.g., Lin et al., 2020; Hua et al., 2020; Pal and Zhang, 2017), fewer studies have investigated the law of distance decay for bicycling or bike-sharing systems. More importantly, the existing relevant work has several major limitations to be addressed: (1) most studies (e.g., Iacono et al., 2008; Krizek et al., 2007) were conducted based on questionnaire-based survey data with limited geographical coverages and suffered from small samples; (2) existing work ignored the spatial heterogeneity of distance decay using DLBS and thus was inefficient in depicting the divergences in distance decay across different urban contexts; (3) no empirical study has quantitatively explored the potential effects of built environments on the distance decay of using DLBS and empirically revealed the underlying mechanisms of the spatial variations in distance decay. The spatial heterogeneity herein refers to the uneven distribution of distance decay patterns in spatial dimensions and differences in distance decay of using DLBS in different urban areas. More specifically, the distance decay of using DLBS in a region of a city differs from that of another region in the same city. These limitations cause inefficiencies in revealing the spatial interactions using DLBS in different urban contexts and deficiencies in accurately modeling spatial distributions of demands for DLBS.

This study aims to fill the above gaps by investigating the spatial heterogeneity in the distance decay of using DLBS and its influencing factors based on emerging and multiple data resources including large-scale passively collected transaction data from DLBS, online map navigator Application Programming Interface (API), Point of Interest (POI) data, road network data and demographic data. First, the trip trajectories of using DLBS are extracted by leveraging transaction records of DLBS in Shanghai of China and online navigator API techniques. The distance decay functions in different urban contexts are empirically estimated based on the revealed trip trajectories. Second, the influences of different built environment factors on the distance decay of using DLBS are explored by Multiple Linear Regression (MLR), making the best of multivariate data from emerging technology tools. These aim to shed light on the underlying reasons for the spatial heterogeneity of distance decay. Third, an Adaptative Geographically Weighted Regression (AGWR) is further performed for revealing the divergences in the effects of built environment factors on distance decay of DLBS, and provide more accurate modeling concerning the distance decay in various contexts. These findings are expected to improve our understanding regarding the distance decay of human movements by DLBS at a microcosmic scale, which would signally support the sustainable planning, operation, and accessibility of DLBS, as well as positive interactions between improvement of DLBS and land use developments.

The remainder of this paper is structured as follows. Section 2 gives an overview of relevant studies about distance decay and the effects of built environments on the usage of bike-sharing systems. Section 3 introduces the study area and multi-source data used in this study. Section 4 describes the methodology for estimating the distance decay functions, extracting built environment factors, and model specifications of MLR and AGWR. The results and discussions are presented in Section 5, followed by concluding remarks in the last section.

2. Literature review

This section reviews two strands of studies that are related to the topics of this study: the law of distance decay in the spatial interactions of human movements and the influences of built environment factors on bike-sharing usages.

2.1. Distance decay of spatial interactions

Distance decay indicates the effect of distance on the intensity of spatial interactions of human movements (Yang et al., 2019). More precisely, the distance decay reflects how the travel demand changes with the traveling distance. It is an important component for travel demand predictions and evaluating the accessibility to various services in urban contexts (Zhu et al., 2020; Yang et al., 2019; Arranz-López et al., 2019). On account of its bearings on modeling spatial distributions of traveling demands, empirical studies have estimated the distance decay functions for different transport modes and different travel purposes based on different types of data. The distance decay pattern noticeably differs across transport modes (e.g., car, public transit or walk) and trip purposes (e.g., work and entertainment) due to the divergences in traveling speeds and value of time for different activities (Arranz-López et al., 2019; Hipp and Boessen, 2017; Iacono et al., 2008). Prior studies have developed different specifications to model the law of distance decay, but the

exponential and power functions are the most prevalent forms (Li et al., 2020; Yang et al., 2019; Halás et al., 2014; De Vries et al., 2009). The conventional approach for estimating distance decay functions used travel survey data such as household travel surveys and travel dairies (e.g., Hipp and Boessen, 2017; De Vries et al., 2009; Iacono et al., 2008; Krizek et al., 2007), which were commonly collected via the resource- and time-consuming approaches such as questionnaires and interviews. This limited the geographical and demographic coverage of samples, so this type of data was hard to be utilized for exploring the law of distance decay in a comprehensive view. With the development of information and communication technology, large-scale datasets concerning spatiotemporal human movement trajectories become available from multiple sources such as GPS data, transport network companies, mobile data, and social media data. Leveraging the emerging data, researchers gain the opportunities to address the traditional issues about distance decay owing to limited samples. Some studies have re-estimated the distance decay functions of different transport modes and trip purposes, and calibrated the typical spatial interaction models using more adequate datasets (e.g., Siła-Nowicka and Fotheringham, 2019; Yang et al., 2019; Arranz-López et al., 2019; Han et al., 2018; Kong et al., 2017). However, most of these extant studies focused on the distance decay of motorized transport modes such as the private car, taxi, and public transit, probably due to the abundance of the data about these modes and their applications in land use and transport infrastructure planning. Similar studies on the law of distance decay of non-motorized alternatives such as bicycling or bike-sharing systems are comparatively rare.

Although several studies have investigated the usage characteristics of bike-sharing systems such as the regional demand (e.g., Lin et al., 2020; Hua et al., 2020; Pal and Zhang, 2017) and usage patterns (e.g., Chen et al., 2020; Barbour et al., 2019), they have focused on modeling the usage amount in an area and provided few insights into the law of distance decay of using DLBS. Few studies concerning the law of distance decay for bicycling or bike-sharing systems could be found. Iacono et al. (2008) conducted one of the early studies for investigating the distance decay pattern of bicycling. They used the travel survey data collected by the University of Minnesota in 2006 to estimate the distance decay functions of bicycling for different purposes including work, shopping, school, entertainment, and trail access. Their results suffered from limited sample sizes, as reported by themselves. Yasmin et al. (2010) investigated how far people were willing to cycle to different destinations in Montréal, Quebec, Canada. They provided empirical results about distance decay of using bikes for work, school, shopping, and leisure based on travel survey data, and indicated that the distance decays for work and leisure trips were less pronounced than those for shopping and school. Lovelace et al. (2017) investigated how the mode share of bicycling changed with travel distance based on a dataset from the UK. However, they only analyzed the distribution of mode share of bicycling in different trip distances but did not empirically estimate the distance decay function of using bikes. Kou and Cai (2019) is the only work that investigated the distance decay for bike-sharing systems on the basis of adequate revealed trip data. They analyzed the distributions of trip distance and duration for using docked bike-sharing systems (DBS), as well as the distance decay functions based on transaction data in eight cities of the USA. Two different travel purposes including commuting and tourism were examined. They concentrated on testing the optimal forms (including Weibull, gamma, and lognormal) for fitting the distributions of distance and duration trips, and indicated that both the distance and duration decay functions of using DBS displayed as a power law.

Through the review, it can be found that the distance decay patterns of using DLBS are lack of comprehensive investigation based on adequate datasets covering different urban contexts. More importantly, the distance decay in different urban contexts was regarded as homogeneous without considerations of potential spatial variations. The built environment factors such as land use characteristics and road infrastructures are declared to have significant influences on travel behavior and patterns of spatial interactions (Gao et al., 2020, 2021; Kang et al., 2013; Yang et al., 2019), and thus may lead to different distance decay patterns of DLBS. However, the spatial heterogeneity of distance decay of using DLBS and its relationships with built environments are not clearly and empirically investigated. The spatial heterogeneity in this study denotes the variances of distance decay in geography and the differences in the distance decay of using DLBS in different urban areas. This study aims to fill these gaps based on a large-scale analysis in Shanghai of China to effectively support the planning and management of DLBS in different urban contexts.

2.2. Effects of the built environment on usages of bike-sharing systems

The built environments refer to the human-made environments that provide settings for human activities, and encompass all forms of buildings (e.g., residential, industrial and commercial), economic infrastructures (e.g., transport infrastructure and park), urban space and landscapes around buildings and infrastructures. Cervero et al. (2009) categorized the various built environment factors into five dimensions including Density, Diversity, Design, Destination and Distance, which are commonly abbreviated as 5-D built environment factors (Cervero et al., 2009). Detailed definitions for the 5-D built environment factors are available in the relevant literature (Cervero et al., 2009; Van Wee, 2002; Cervero and Kockelman, 1997). It is widely recognized that built environments have significant influences on shaping the patterns of human mobility and activities. Some studies have explored the effects of built environment factors on the usages of both docked and dockless bike-sharing systems, taking advantage of the emerging data resources produced by bike-sharing systems. More specially, the relevant studies have examined the effects of built environments on the usage demand (e.g., El-Assi et al., 2017; Zhang et al., 2017), temporal usage patterns (e.g., Ji et al., 2020; Liu and Lin, 2019; Bao et al., 2017), and usage dynamics such as variances in the trip distance, time and speed (e.g., Kou and Cai, 2019; Mateo-Babiano et al., 2016). For instance, El-Assi et al. (2017) executed a spatial analysis of the effects of built environments on the usage demands of bike-sharing systems in Toronto. Their results demonstrated that the bicycling infrastructure, temperature, and land use characteristics significantly correlated with the amount of bike-sharing trips. Liu and Lin (2019) examined the associations between built environments and temporal usage patterns of docked bike-sharing systems in Taiwan. The temporal patterns were defined as the demand fluctuation of each bike-sharing station in time series. The temporal usage patterns of all stations were classified into four categories using a hierarchical clustering method. A multinomial logit regression was employed to model the correlations between built environment factors and classified
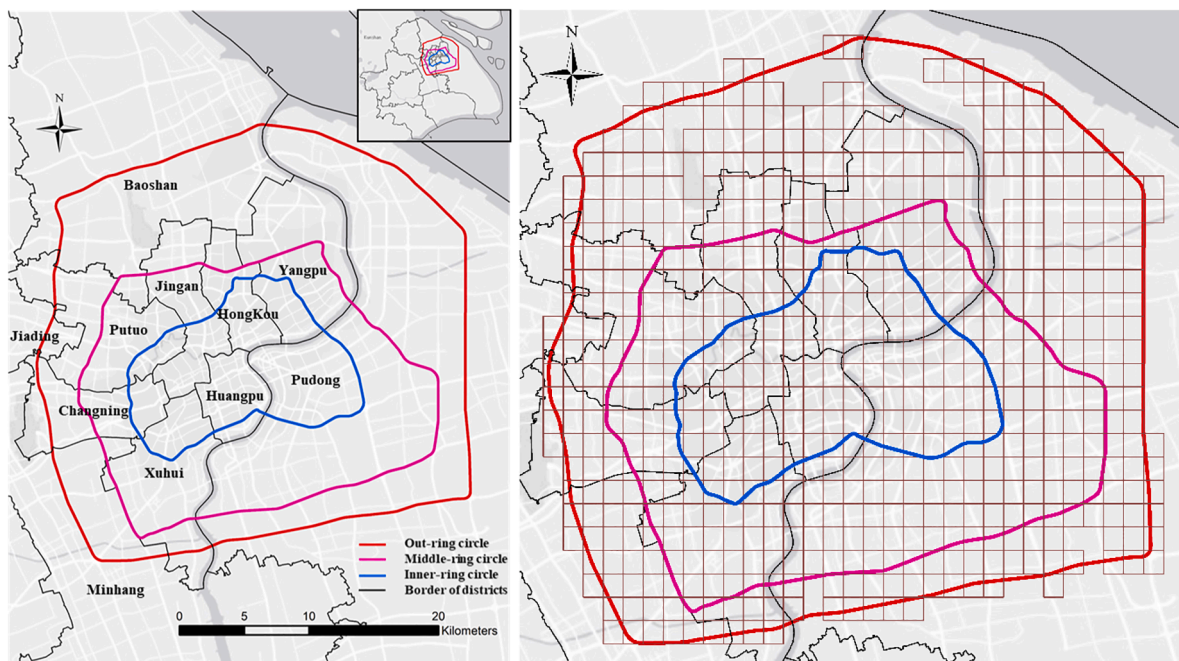
Fig. 1. The studied area and partitioned analysis zones.

temporal patterns. Moreover, most of the aforementioned studies were based on data from docked bike-sharing systems which had fixed stations. The docked stations restrict the origin and destination of trips using docked bike-sharing systems, and thus reduce the users' accessibility and flexibility of using shared bikes. For instance, the user has to walk from the origin to a starting station for picking up and walk for an ending station to her/his final destination; the user can not using bikes in a docked bike-sharing system to a place without parking stations around it for one-way trips. In contrast, DLBS allows users to pick-up and drop-off likes anywhere in service zones, and provides more convenient and flexible services. The distinctions in DLBS and docked bike-sharing systems could lead to different usage patterns (Lazarus et al., 2020) and may influence the distance decay patterns as well. In this study, we focus on DLBS on account that it is more prevalent and more likely to be the future trend.

Differing from existing literature that focused on the usage demands for bike-sharing systems in an area, this study concentrates on the law of distance decay of using DLBS. The distance decay focuses on how the intensity of mobility flow reduces with distance, which is a different aspect in contrast to demand in an area. As far as we are concerned, no existing work has investigated the effects of built environment factors on the distance decay of using DLBS, despite the distance decay is an indispensable element for effective planning and management. Thus, this study endeavors to decipher the associations of 5-D built environment factors with the distance decay of using DLBS, which will help to reveal the underlying mechanism of spatial heterogeneity in the distance decay of using DLBS and accurate modeling of spatial interaction using DLBS.

3. Study areas and data resources

This study utilizes the transaction data of DLBS in Shanghai of China provided by Mobike company (https://mobike.com/) for our analysis. Mobike is one of the biggest unicorn companies about micro-sharing mobility in China. Shanghai is one of the largest megacities in the world with a population of around 24.24 million and a municipal area of 6341 km^2 in 2019. The municipal area of Shanghai is demonstrated in Fig. 1. In addition, Shanghai is one of the largest bike-sharing markets around the world, which has over 1 million publicly sharing bikes by the end of 2017. The used dataset covers 27,238,412 trip transactions recorded by 635,875 publicly sharing bikes (taking up around 40% bike-sharing market of Shanghai[1]) in 14 continuous days from August 26th to September 8th in 2018. The large quantity of data and the contexts of Shanghai guarantee the representativeness of the used dataset. In this study, we select the urban space inside the out-ring circle of Shanghai (i.e., the red line in Fig. 1) for investigations on account that the transactions out of the area are sparse and maybe not adequate for reliable analysis. The size of the studied area is 667.3 km^2, which covers (or partly covers) 11 administrative districts in Shanghai, including Changning, Hongkou, Xuhui, Putuo, Pudong, Baoshan, Huangpu, Minhang, Yangpu, Jingan, and Jiading district. The studied area contains various urban contexts including urban regions, suburban regions, rural areas, and rural–urban continuums. The purple and blue lines represent the middle-ring circle and inner-ring circle in Shanghai, respectively. The regions inside the inner-ring circle are the downtown areas of Shanghai. The areas outside the out-ring are

---

[1] Information from https://baijiahao.baidu.com/s?id=1603972856220492265&wfr=spider&for=pc.

(a)

(b)   (c)
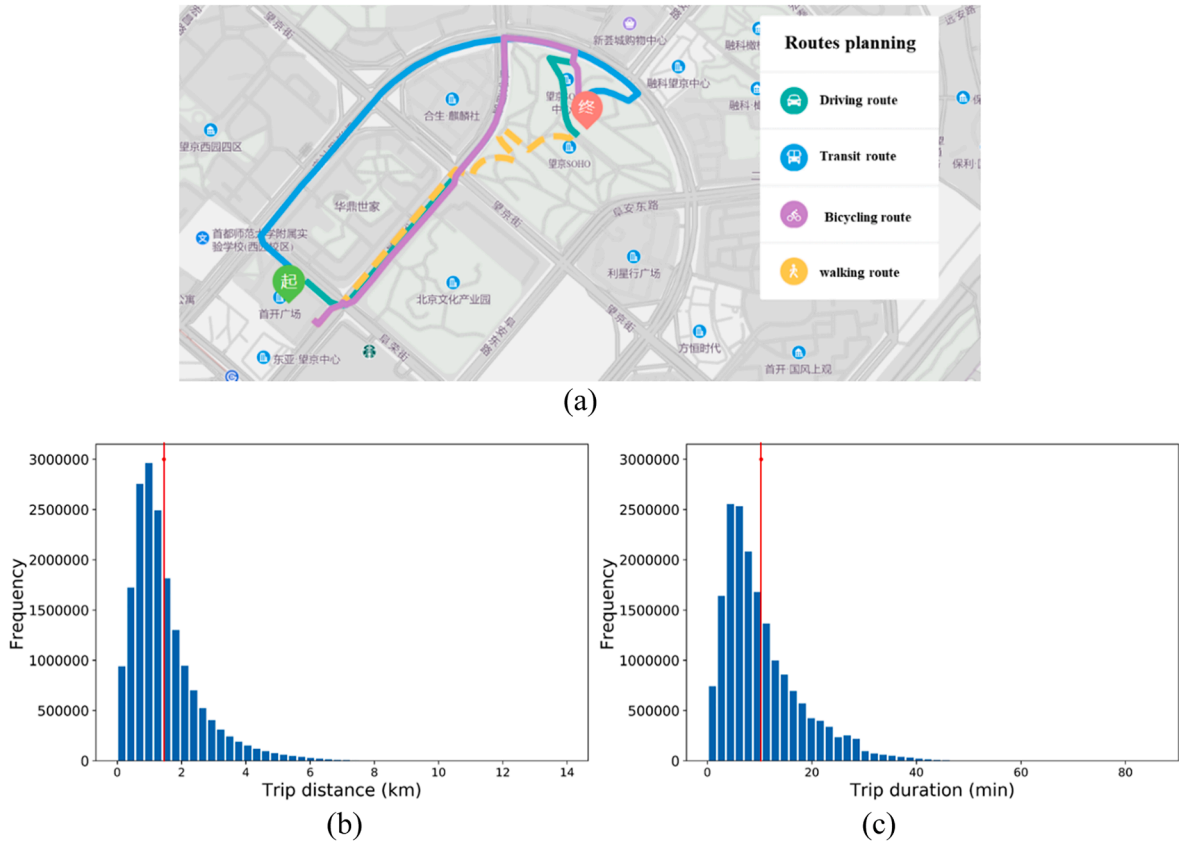
Fig. 2. (a) Routing API in Amap, (b) the trip distance distribution, and (c) the trip duration distribution.

generally regarded as suburban or rural regions of Shanghai. The area between inner-ring and out-ring has both urban and suburban regions. The study area is divided into a grid with $0.01°$ (latitude) $\times 0.01°$ (longitude) rectangles and each rectangle is an analysis zone (AZ)[2], as demonstrated in Fig. 1. To ensure the reliability of the analysis, several AZs are excluded in preprocessing as they have comparatively fewer records (less than 5000 records in the two weeks) and maybe not reliable for analysis. The excluded AZs are mostly covered by elements such as rivers, ports, or planting bases and thus have fewer records. Finally, 620 AZs are selected for analysis, as shown in Fig. 1.

Each transaction record consists of the transaction ID, bike ID, the starting and ending locations of the trip (latitude and longitude), the starting and ending timestamps. To acquire the riding distance of each trip, much literature (e.g., Liu and Lin, 2019) directly calculated the Euclidean distance between starting and ending locations, due to the difficulty of obtaining the riding route based on the starting and ending points. This is apparently not accurate and results in biases of riding distance. The actual riding distance of each trip is expected to larger than the Euclidean distance between starting and ending locations in most cases on account of road network structures. The riding route and distance highly depend on travel contexts such as road topology and density. To obtain plausible riding distance of each trip, we take advantage of the route planning API of the online navigation platform Amap[3] to extract the recommended riding route between the starting and ending locations. The Amap navigation platform is one of the most prevalent and frequently used online navigation tools in China, so we believe that the recommended riding route is the one that most people would adopt in reality. By utilizing the API developer port provided by Amap, we use the Python programming to extract to riding routes of all trips. The outputs contain the trajectory of the recommended riding route and distance of each trip, in which we can attain the plausible riding distance for each trip. An example of the API interface is illustrated in Fig. 2(a).

The devices on the sharing bikes have a very low probability of showing technical errors (e.g., position drifting of GPS). We observed that the recorded locations have abnormal values in some rare and extreme cases. This results in wrong trip information (e.g., extremely long riding distance and high riding speed). Therefore, we set three criteria to filtrate the outliers: 1) the riding distance should be less than 30 km; 2) the riding duration should be less than 1 day; 3) the average speed of the trip should be in the range from 2 to 25 km/h (Li et al., 2020). Transactions that do not meet the above criteria are excluded from the datasets. After data cleaning,

---

[2] The area of a partitioned analysis zone $(0.01°$ (latitude) $\times 0.01°$ (longitude)) is around 1.11 km $\times$ 0.96 km = 1.07 km^2.
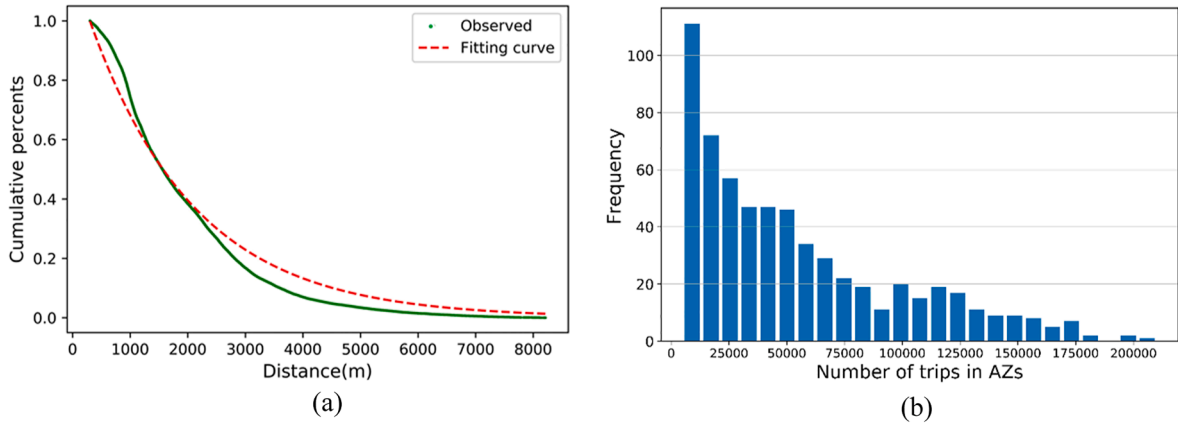[3] https://lbs.amap.com/api/webservice/guide/api/direction.

Fig. 3. (a) the distance decay functions and (b) the distributions of the number of trips for fitting the functions in AZs.

16,977,889 transactions in the above 620 AZs have used for final analysis. The distributions of trip distance and duration of all trips are demonstrated in Fig. 2(b) and (c), respectively. Most trips are less than 6 km and 40 min. The average trip distance and duration demonstrated by red lines in Fig. 2(b) and (c), are 1.45 km and 10.2 min, respectively. These basic statistics are in line with the results reported by the relevant literature (e.g., Li et al., 2020; Kou and Cai, 2019).

As for obtaining the built environment factors in each AZ, another three datasets from multiple sources are utilized. The first dataset is about POI obtained from the POI API of Amap platform.[4] The database provides all POIs in the area of Shanghai and contains 1,120,924 POIs. Each POI data consists of the element name, address, element types, and their locations (longitude and latitude). There are 44 types of POI defined by Amap to demonstrate different utilization purposes such as entertainment, restaurant, education, and enterprise. The list of POI categories is demonstrated in Table A.1 (in the appendix). The detailed descriptions about the categories are available on the Amap website.[5] As per the POI, we further categorize them into six categories of land-use types for analysis based on the land use classification standards in China. The matchups between the categories in this study and the POI categories from Amap are shown in Table A.1. The investigated land-use types consist of commercial land use, living land use, public management and service land use, industrial land use, road and transport infrastructure land use, and park and square land use. By mapping the POIs into the partitioned AZs, the number of different categories of POI in each AZ can be extracted and utilized to calculate the land use characteristics and transport-related elements (e.g., parking lots, metro and bus stations) in each AZ. The second dataset is the GIS information about detailed road networks provided by OpenStreetMap. The dataset is utilized to collect the density of road infrastructure in each AZ such as the density of different road classes. The third dataset is the population data in Shanghai to obtain the population density in each AZ, which is based on the Sixth National Census of China.

4. Methodology

4.1. Estimating the distance decay functions

The distance decay depicts the principle that mobility flows decrease along with travel distance. The distance decay function could be estimated by fitting a continuous relationship of the cumulative percentages of trips with corresponding trip distances, as illustrated in Fig. 3(a). For instance, the point (0.7, 1000) denotes that 70% of trips using DLBS in the area have a riding distance larger than 1000 m. Different forms have been proposed to represent the law of distance decay, but power and exponential functions are preferred by most relevant studies (Li et al., 2020; Yang et al., 2019; De Vries et al., 2009). This study adopts the exponential form to model the distance decay of using DLBS for each AZ after empirical comparisons of the two functions. The equation of distance decay function is:

$$P(x) = \begin{cases} 1 & x \leqslant a \\ e^{-\beta \cdot (x-a)/1000} & x > a \end{cases} \tag{1}$$

where $P(x)$ is the cumulative percentage of trips that have a riding distance larger than x meters. On account that the law of distance decay is only sensitive when the trip distance exceeds a threshold, we do not use the data with riding distances less than 300 m (i.e., a = 300) to eliminate its effects on the fitting results referring to Li et al. (2020). The coefficient of distance decay β indicates how fast the flows of spatial interactions using DLBS decrease with trip distance and is estimated based on real observed trip data in each AZ. For each AZ, the trips whose origins or destinations fall into the AZ, are selected as the data for estimating its distance decay function. Based on the statistics of trip distances of all trips in an AZ, the observed cumulative percentage curve of trip distances using DLBS for

---

[4] https://lbs.amap.com/api/webservice/guide/api/search.
[5] https://lbs.amap.com/api/webservice/download.

Table 1
The built environment variables and definitions.

Explanatory variables	Definitions	Unit
Density		
Population density	Number of residents in each AZ	persons/km^2
Employment density	Number of employment positions in each AZ	number/km^2
Diversity		
Commercial land use ratio	The floor area of the commercial/business use divided by the floor space in each AZ	%
Living land use ratio	The floor area of the living land use divided by the floor space in each AZ	%
Public management and service land use ratio	The floor area of the public service land use divided by the floor space in each AZ	%
Park and square land use ratio	The floor area of the park and square land use divided by the floor space in each AZ	%
Industry land use ratio	The floor area of the industrial land use divided by the floor space in each AZ	%
Land use entropy	The land use entropy is an indicator for measuring the degree of land use mix (Zhang and Zhao, 2017; Cervero, 1988). It is calculated by $\frac{-\sum_{i=1}^{K} R_i \cdot \ln(R_i)}{\ln(K)}$, $\sum_{i=1}^{K} R_i = 1$ where R_i is the ratio of land use type i and K is the total number of all land use types	
Design		
Motorway density	The length of motorway including the arterial and motorway that not allow bicycling in each AZ	m/km^2
Motorized road density	The length of primary and secondary roads that can be used by bicycles but prioritize motorized vehicles in each AZ	m/km^2
Branch road density	The length of street, service and living roads in each AZ	m/km^2
Bicycle lane density	The length of dedicated lanes for bicycles in each AZ	m/km^2
Destination		
Leisure facility density	The density of leisure facilities, and calculated by the number of POIs whose code is in {20, 21, 22, 23, 24, 25, 26, 27, 28, 29, 31, 32, 34, 37, 38, 39, 41} in Table A.1 for each AZ	number/km^2
Education facility density	The density of education-related facilities and calculated by the number of POIs belonging to the category of school and education institutions in Table A.1 for each AZ	number/km^2
Park and square density	The density of park and square, and calculated by the number of POIs belonging to the category of park/square in Table A.1 for each AZ	number/km^2
Distance to transit		
Metro station density	The number of metro stations in each AZ based on POI datasets divided by the floor area	number/km^2
Bus station density	The number of bus stations in each AZ based on POI datasets divided by the floor area	number/km^2
Parking lot density	The number of parking lots in each AZ based on POI datasets divided by the floor area	number/km^2

the AZ could be acquired, namely the green point line in Fig. 3(a). The least square method is utilized to fit the Eq. (1) for estimating the coefficient of distance decay β for each AZ. The distributions of the number of trips for estimating the distance decay functions of above 620 AZs are illustrated in Fig. 3(b). The minimum number of trips for fitting the distance decay function is 5019 and most AZs have over 10,000 trips, which are sufficient for reliable model estimations.

4.2. Built environment variables

To explore the effects of built environments on the distance decay for DLBS, we collect various built environment factors from multiple data sources. We follow the framework of the 5-D built environment factors proposed by Cervero et al. (2009) including Density, Diversity, Design, Destination, and Distance to transit. The adopted built environment factors in each dimension are based on our available datasets and cover most built environment factors that were reported to influence the travel behavior in the literature (e. g., Liu and Lin, 2019; Ji et al., 2020; Bao et al., 2017). Definitions and calculating methods of used built environment factors are listed in Table 1. These variables were measured within each AZ separately.

The population density is calculated based on the Sixth National Census of China. However, the used surveying zone in population census is not in accord with the partitioned AZs in this study. Therefore, this study calculates the population density in each AZ as per the overlapping areas between the AZs and population census survey zones (Yang et al., 2019; Yin et al., 2015). The formula is:

$$PD_i = \sum_{m=1}^{M} \frac{O_{im}}{S_i} \cdot PD^m \tag{2}$$

where PD_i is the population density of AZ i, O_{im} is the overlapping areas of AZ i and population census zone m, S_i is the area of AZ i, and PD^m is the surveyed population density in the census zone m. The employment density is surrogated by the density of POIs that can provide jobs including POIs representing commercial service and public management and service in Table A.1.

For obtaining the land use characteristics in each AZ, most literature directly uses the number of POIs of different categories to represent the land use ratios of different categories (e.g., Bao et al., 2017; Sun et al., 2017). This is not accurate as the land use ratio is defined as the floor area for a certain land use divided by the total floor space in an area. The number of POIs can merely measure the
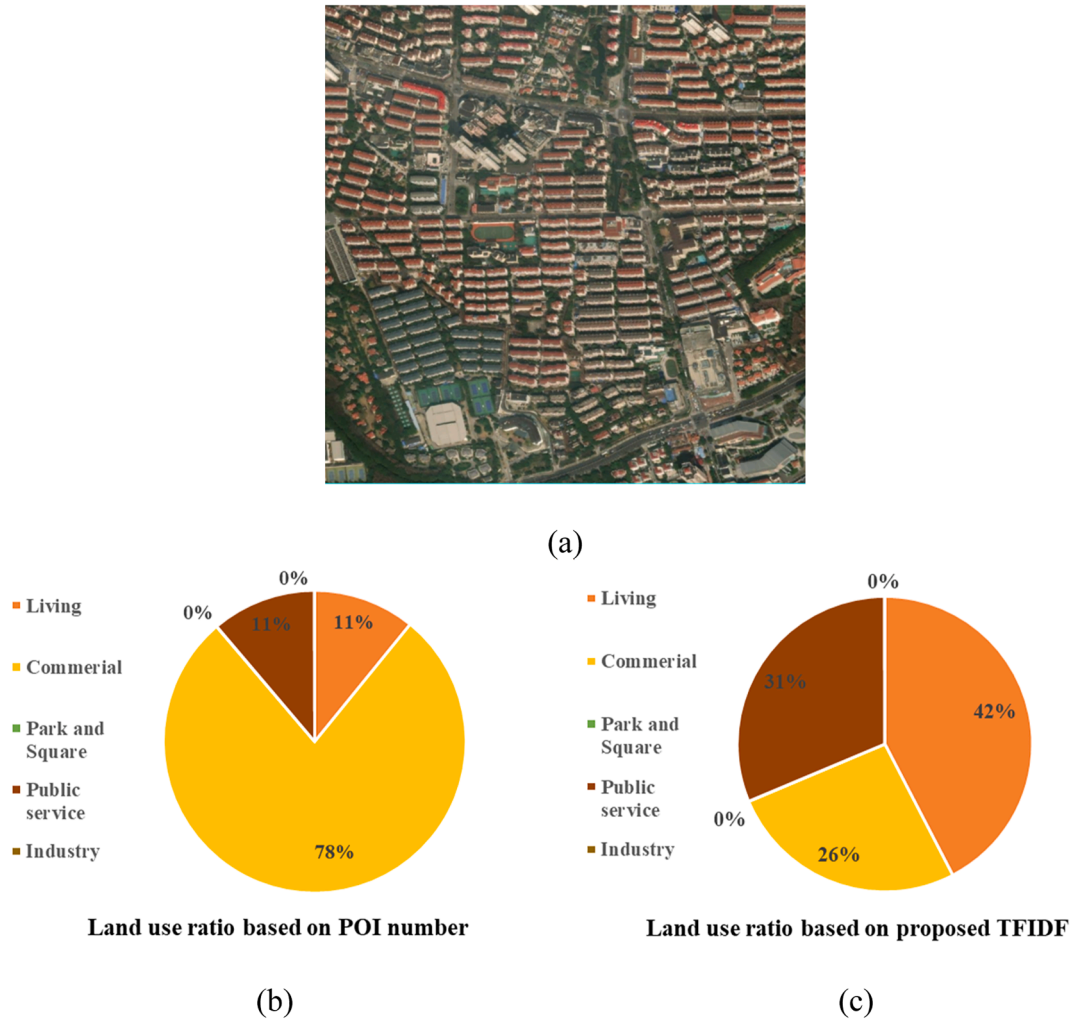
(a)

Land use ratio based on POI number

Land use ratio based on proposed TFIDF

(b)

(c)

Fig. 4. An illustrative example of the proposed TFIDF method for characterizing the land use ratios. The displayed area has 354 POIs about living land use (as defined in Table A.1 in appendix), 2536 POIs about commercial land use, 1 POI about park and square land use, 364 POIs about public management and service land use, and 1 POI about industrial land use.

number of services, while it cannot directly represent the floor areas for different land use categories. More importantly, the amount of POIs in different categories provided by the online map is often highly imbalanced. For instance, a residential community only has several residential POIs, but has a lot of commercial POIs as many commercial services commonly exist around the living communities. If we directly use the amount of POIs for measuring different land use ratios, a residential community could be measured to have a high commercial land use ratio, rather than a high residential land use ratio. Therefore, the imbalance feature of POIs of different categories may lead to biases in calculating land use ratios. To amend the imbalance features of POI data from online maps, we take advantage of a topic modeling method from the field of information retrieval to calculate the ratios of different land use in each AZs. Term frequency-inverse document frequency (TFIDF), is a numerical statistic model customized to reflect how important a word is to a document in a collection or corpus (Hakim et al., 2014). In TFIDF, the importance of a certain word in a document increases proportionally to the number of times the word shows up in the document, and the weight of the word is related to the frequency of the word in all documents of the corpus, which is designed to rectify the fact that some words appear more frequently in general. In our case, each AZ is analogous to a document and has a variety of POIs, each of which is analogous to a word in the document. All AZs could be regarded as documents in a corpus (namely a city). The aim is to obtain the degree of a certain category of POI (e.g., commercial POI) in each AZ, which is analogous to the importance of a certain word in a document for topic modeling. As per TFIDF, the degree of a category of POI in an AZ can be obtained by:

$$tdidf_{ki} = td_{ki} \cdot idf_k$$

$$td_{ki} = \frac{N_{ki}}{\sum_{k=1}^{K} N_{ki}}$$

$$idf_k = log\frac{\sum_{i=1}^{D} N_{ki}}{\sum_{i=1}^{D}\sum_{k=1}^{K} N_{ki}}$$

(3)

where td_{ki} is the term frequency of POI category k, N_{ki} is the number of POIs belonging to POI category k in AZ i, K is the number of POI categories in AZ i, idf_k is the weight of POI category k, and D is the number of AZs in the study area. Afterward, the ratio of the land use category k can be calculated by:

$$R_{ki} = \frac{tdidf_{ki}}{\sum_{k=1}^{K} tdidf_{ki}}$$

(4)

where R_{ki} is the ratio of land use type k in AZ i. Based on this approach, we can acquire the ratios of different land-use types listed in Table 1. Five types of land use are considered in the final analysis as per the generally adopted land use classifications in China, including commercial service land use, living land use, public management and service land use (e.g., administrative institutions, education, and hospital), park and square land use, and industrial land use. The road and transport infrastructure land use are not considered as similar variables such as road density and transit station density have already been incorporated in the factors concerning design and distance to transit. Fig. 4 demonstrates an example of the difference between using the proposed TFIDF and the traditional methods (i.e., directly use the POI number for characterizing the land use ratios) in calculating the land use ratios in an area. Fig. 4(a) displays the satellite view of an area in Shanghai. It can be easily identified from map that this area is mainly covered by residential buildings (namely large living land use ratio) and has some life services (e.g., shops) in the area. If the land use ratios are calculated based on the number of different POIs, the results are shown in Fig. 4(b), which are apparently not in line with the observed land use in the area due to imbalance features of POI data. The results based on the proposed TFIDF are shown in Fig. 4(c) and reflect the real land-use characteristics much better as compared to traditional methods.

The explanatory variables about design in Table 1 are calculated by mapping the road network from OpenStreetMap with the partitioned AZs, taking advantage of the interacting tools in ArcGIS. For the explanatory variables about destination and distance to transit, they are calculated by mapping the POI data into the partitioned AZs and get the statistics of different POI categories in each AZ as described in Table 1. For explanatory variables concerning distance to transit, we intend to obtain the average distance to transit facilities such as metro and bus stations. On account that all AZs have similar acreages, the number of transit facilities in each AZ is applied as the indicators of the average distance to transits.

4.3. Modeling the effects of built environments on the distance decay of DLBS

To investigate the effects of built environment factors on the distance decay of using DLBS, we firstly use a Multiple Linear Regression method to model the relationship between the distance decay coefficient (i.e., β) and different explanatory variables. The formula of MLR is

$$Y_i = \alpha_0 + \sum_{l=1}^{L} \alpha_l x_{li} + \varepsilon_i$$

(5)

where Y_i is the distance decay coefficient in AZ i, x_{li} denotes the explanatory variable in AZ i, α_l and α_0 are the coefficients of variables and the intercept to be estimated respectively, and ε_i is the random residual error. The MLR model is estimated by Ordinary Least Squares approach. Before the formal regression, we check the potential multicollinearity among explanatory variables, which may result in noticeable biases in the estimation. The variance inflation factors (VIF) of all explanatory variables are calculated. The variables with a VIF larger than 5 are excluded and remaining variables all have a VIF less than 4. The employment density and living land use ratio are excluded due to multicollinearity with other variables. Based on the estimation results, the built environment factors that have significant effects on the distance decay coefficient could be identified and the global effects of built environments on distance decay of using DLBS could be revealed.

However, the estimated coefficients in MLR are identical and constant for all AZs due to the globalism of this model. Thus, the potential variance in the effects of built environment factors on distance decay is not fully addressed. Simultaneously, the law of distance decay of using DLBS for each AZ is not merely dependent on the built environment in the AZ, but also relates to the built environment in the surrounding AZs. The MLR is not sufficient to reflect the effects of built environments in adjacent AZs due to its globally average characteristics. To solve the two problems, we further use an advanced method Adaptative Geographically Weighted Regression for analysis. AGWR is a powerful method for spatial analysis and is superior in detecting local variations that may be covered by global regression models (Zhou and Lin, 2019; Brunsdon et al., 1996). In AGWR, the coefficients of built environment factors are fitted for every AZ to obtain local parameter estimates instead of global estimates (Yang et al., 2019; Brunsdon et al., 1996). The formula of AGWR is
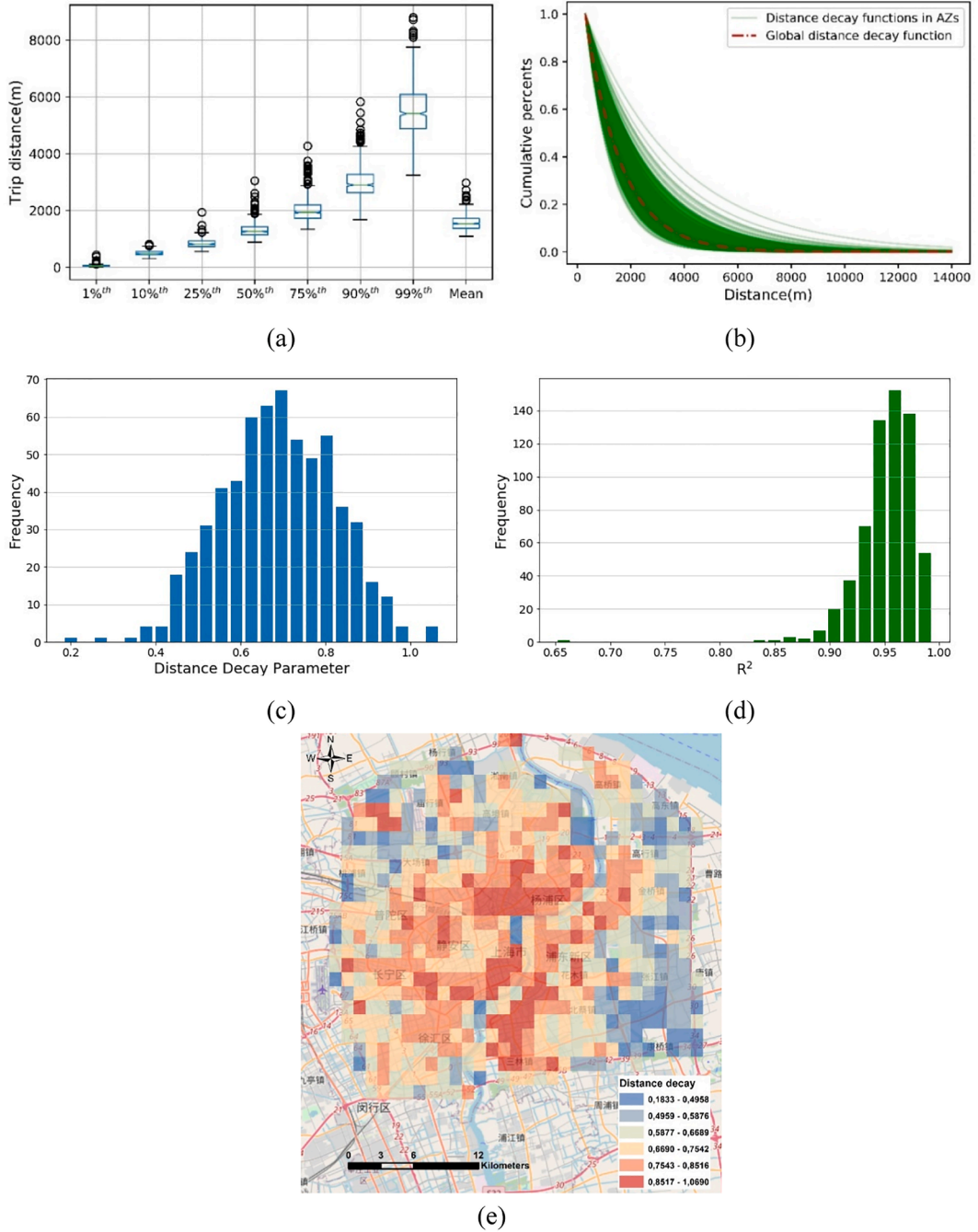
Fig. 5. (a) The quantiles of trip distance distributions, (b) the distance decay functions, (c) the coefficients of distance decay, (d) the R-squared values of fitting distance decay functions, and (e) the coefficients of distance decay in urban space.

$$\mathbf{Y} = (\alpha \otimes \mathbf{X}) \cdot \mathbf{A} + \varepsilon \tag{6}$$

where $\otimes$ is the multiplication operator to calculate the multiplication of each element in $\mathbf{X}$ and α. $\mathbf{X}$ and α are the explanatory variable matrix containing the built environment factors in all AZs and the corresponding coefficient matrix, respectively. For a case that has D analysis zones and L explanatory variables in each zone, $\mathbf{X}$ and α have $D \times (L+1)$ dimensions. $\mathbf{A}$, of which elements are all 1, is $(L+1) \times 1$ matrix for calculating the $\mathbf{Y}$. $\mathbf{Y}$ and ε are the $D \times 1$ matrixes for the dependent variable and residual error, respectively. The coefficients of each analysis zone are estimated by the weighted least squares method as shown below:

$$\alpha_i = (\mathbf{X}^T\mathbf{W}_i\mathbf{X})^{-1}\mathbf{X}^T\mathbf{W}_i\mathbf{Y}$$

$$\mathbf{W}_i = \begin{bmatrix} w_{i1} & 0 & ... & 0 \\ 0 & w_{i2} & ... & 0 \\ ... & ... & ... & ... \\ 0 & 0 & ... & w_{iD} \end{bmatrix} \tag{7}$$

where $\mathbf{W}_i$ is a $D \times D$ spatial weighting matrix, in which the off-diagonal elements are zeros and diagonal elements are the geographical weights for estimating the coefficients in AZ i. The basic mechanism of AGWR is obtaining separate regression results for each analysis zone, in which the influences of adjacent areas are inversely proportional to the distance to the center of the analysis zone i. The popular Gaussian kernel function is adopted herein to obtain the spatial weighted matrix within a certain bandwidth. The bandwidth denotes the considered areas for each local regression equation. The selection of bandwidth has significant effects on the estimation results (Yang et al., 2019; Brunsdon et al., 1996). We select the optimal bandwidth for each analysis zone based on minimizing the value of the Akaike Information Criterion (AICc) and in an adaptative manner. The adaptative manner means different analysis zones have different bandwidths. In the estimations of MLR and AGWR, all the explanatory variables are standardized by using the z-score method to eliminate the influence of magnitudes of different factors and ensure the stability of estimation (Yang et al., 2019). The MLR is regressed using Python statistical packages and the AGWR model is estimated using ArcGIS 10.5.

5. Results and analysis

5.1. Spatial heterogeneity of distance decay characteristics of DLBS

Taking advantage of the extracted AZ-based trips, we first compared the distributions of trip distance in different AZs. The statistics about the quantiles of trip distance distributions across all AZs are shown in Fig. 5(a). The mean trip distance is a little bit larger than the 50% quantile. This indicates the distributions of trip distance present right skewness, which is in accord with other empirical findings (Li et al., 2020; Kou and Cai, 2019). It can be observed that there are obvious variations in the quantiles of trip distance distributions across different AZs, implying the trip distance patterns in different AZs indeed differ from each other. We estimated a global distance decay function using all data in the study area without distinguishing different AZs. It is demonstrated by the red line in Fig. 5(b). The estimated global distance decay coefficient (i.e., β in Eq. (1)) of using DLBS is 0.7421. The larger the distance decay coefficient is, the more pronounced travel distance influences the percentage of travel demand (namely intensity of mobility flows). As compared to the distance decay coefficient for motorized transports in relevant literature such as 0.15 in Martínez and Viegas (2013) and ranging from 0.01 to 0.35 in Halás et al. (2014), the distance decay coefficient of using DLBS is noticeably larger, indicating the travel demand using DLBS is much more sensitive to trip distance compared to motorized modes such as car and transits. It is anticipated because bicycling is mainly targeted at short-distance trips. With increasing trip distance, the willingness to use DLBS should decrease more conspicuous as compared to motorized modes. This confirms the necessity of distinguishing the distance decay of using DLBS with other transport modes.

For each AZ, the distance decay function is estimated. The fitted distance decay functions for all AZs are illustrated in Fig. 5(b) by green lines. Fig. 5(c) and (d) further demonstrate the statistics regarding estimated distance decay coefficients for all AZs and corresponding goodness of fit. The goodness of fit is mostly greater than 0.85, meaning the used exponential functions can nicely fit the law of distance decay of using DLBS. More importantly, we can observe notable divergences in the estimated distance decay functions across AZs. The distribution of distance decay coefficients shows a Gaussian normal distribution, in which most values fall into the range from 0.4 to 1. The law of distance decay in some AZs evidently diverges from the global distance decay function, as shown in Fig. 5(b). As per the results, it can be concluded that the distance decay of using DLBS is not homogeneous for the entire city but varies notably. Fig. 5(e) projects the estimated distance decay coefficients of using DLBS in the study area. Obvious spatial heterogeneity in the distance decay coefficients could be observed. More importantly, the distance decay coefficients of AZs show agglomeration or clustered patterns in the spatial dimension. Namely, the AZs that close to each other have similar distance decay coefficients. We employ the global Moran's I index to test the spatial autocorrelation of distance decay coefficients. The result gives a Moran's I index of 0.5942 (z-value: 20.126 and p-value: 0.000), demonstrating significant correlations of distance decay coefficients in spatial space. From the perspective of spatial dimension, the flows of spatial interactions using DLBS in the AZs located in the downtown areas reduce more sharply with increasing distance (i.e., higher distance decay coefficient) than those far from the downtown area, especially in the southeast part (namely south part of Pudong district of Shanghai). The land-use intensity and entropy in the downtown areas of Shanghai are much higher than those in suburban or rural areas. People can access to various services in a short distance. Simultaneously, the downtown has a high density of public transit facilities and is more convenient to use transits such as metro and bus to diverse destinations. As a result, travelers may be apt to use public transits to reach transit stations near their destinations and then use DLBS or walk to the final destinations, which would result in more short-distance trips of using DLBS. These are potential explanations for the larger distance decay in the central areas in contrast to suburban areas. Besides, the difference also implies the potential correlations between the distance decay of using DLBS and the built environment in different urban contexts.

5.2. Effects of built environments on distance decay of using DLBS

To examine the effects of built environment factors on the distance decay of using DLBS, we apply the MLR to model the associations of distance decay coefficient in each AZ with built environment factors. As aforementioned, a multicollinearity check was

Table 2
Results of the MLR model.

Variables	Coefficient	Standard Error (SE)	T-value	P-value	Robust SE	Robust t-value	Robust P-value	VIF
Intercept	0.6887	0.0039	176.9393	0.000**	0.0038	179.4162	0.000**	–
Density								
Population density	0.0504	0.0052	9.6644	0.000**	0.0047	10.8056	0.000**	1.793
Diversity								
Land use entropy	0.0200	0.0049	4.0837	0.000**	0.0054	3.6812	0.000**	1.585
Commercial land use ratio	−0.0175	0.0045	−3.8469	0.000**	0.0048	−3.6254	0.000**	1.359
Public service land use ratio	0.0009	0.0043	0.2073	0.835	0.0047	0.1865	0.852	1.196
Park and square land use ratio	−0.0099	0.0047	−2.1231	0.034**	0.0044	−2.2347	0.026**	1.446
Industrial land use ratio	−0.0236	0.0050	−4.6864	0.000**	0.0062	−3.8275	0.000**	1.680
Design								
Motorway density	−0.0148	0.0040	−3.6731	0.000**	0.0042	−3.5212	0.000**	1.066
Motorized road density	0.0033	0.0046	0.7253	0.468	0.0043	0.7656	0.444	1.374
Branch road density	0.0123	0.0046	2.6817	0.007**	0.0047	2.6177	0.009**	1.384
Bicycle lane density	−0.0008	0.0042	−0.1992	0.8422	0.0040	−0.2112	0.832	1.164
Destinations								
Leisure facility density	−0.0107	0.0069	−1.5482	0.1221	0.0057	−1.8961	0.058*	3.161
Education facility density	0.0106	0.0049	2.1535	0.031**	0.0049	2.1709	0.030**	1.604
Park and square density	−0.0025	0.0050	−0.4876	0.626	0.0043	−0.5694	0.569	1.666
Distance to transit								
Metro station density	0.0145	0.0042	3.4653	0.000**	0.0040	3.6461	0.000**	1.155
Bus station density	0.0026	0.0051	0.5163	0.6059	0.0053	0.4988	0.618	1.708
Parking lot density	0.0193	0.0065	2.9818	0.003**	0.0060	3.2036	0.001**	2.779
Number of observations: 620				Akaike's Information Criterion: −1114,705				
R-Squared: 0.488				Adjusted R-Squared: 0.471				

Note: VIF denotes the variance inflation factor. ** and * represent the significance at the confidence level of 95% and 90%.

executed before regressions. Finally, sixteen explanatory variables remain in the model, all of which have a VIF value of less than 4. The results of the MLR are displayed in Table 2. The estimated model has an adjusted R^2 of 0.471, meaning the selected variables explain 47.1% of the variations in the distance decay coefficients across different AZs.

From a global perspective, several built environment factors are identified to significantly influence the value of the distance decay coefficient at the confidence level of over 95%. It should be noted that the distance decay coefficient reflects the marginal decrease in usage percentages of DLBS with increasing trip distances in an area, as shown in Fig. 3(a). A larger distance decay coefficient means the usage percentages of DLBS reduce relatively faster with increasing distance. The population density is found to be positively related to the distance decay coefficient, indicating AZs with higher population density have larger distance decays of using DLBS. Areas with high population density tend to be residential areas. Residential communities in Shanghai are generally surrounded by matching transit services (e.g., bus/metro stations), living and commercial services such as food shops, small markets, and education facilities. The DLBS in such areas may mainly serve as a flexible tool to access adjacent life services such as shops, markets, and restaurants in nearby areas. For long-distance trips, travelers may choose other modes rather than DLBS. These may lead to the phenomenon that most DLBS trips in these AZs are short-distance and comparatively fewer long-distance trips of using DLBS. These may be the reason for larger distance decay in AZs with more population. This finding is different from the effect of population density on the distance decay of motorized modes reported by Yang et al. (2019), which indicates that a higher population density is linked to lower distance decay. This demonstrates the divergence in the laws of DLBS as compared to motorized modes. For built environment factors about diversity, AZs with higher land use entropy show larger distance decay of using DLBS. A high land use entropy implies balanced land use characteristics in the areas and ensures that people can reach diverse services in short distances. This may result in the phenomenon that most usages of DLBS are short-distance trips, which corroborates the finding of population density. However, the commercial, park and square, and industrial land use ratios are found to be negatively associated with distance decay of using DLBS. An AZ with higher commercial or park and square land use provides attractive life and leisure services, which is likely to attract people on a large scale and lead to lower distance decay of using DLBS. Industrial areas in Shanghai generally contain many factories or manufacturing bases, and have less dense commercial and life services. People in these areas would need to travel comparatively long distances using DLBS for conducting their daily activities such as working, shopping, and connections to nearby transit stations. These might be the reason for smaller distance decay in AZs with a higher industrial land use ratio.

As for the factors about design, a larger motorway road density is significantly linked to smaller distance decay. The motorways in Shanghai are not allowed for bicycling and thus reduce the accessibility of using DLBS to the surrounding destinations, which would force travelers to travel long distances using DLBS due to detours. In contrast, a larger branch road density is significantly associated with larger distance decay of using DLBS. The potential reason could be that branch roads are bicycling friendly, and friendly road environments enhance the usage of DLBS to various destinations in local areas with direct routes and comparatively shorter distances. In our results, we did not identify a significant or substantial correlation between bike-dedicated lanes and distance decay of using DLBS, even though some studies reported that bike-related infrastructures could improve the usage demand of bikes (e.g., Mateo-Babiano et al., 2016). The leisure facility density is found to be negatively related to the distance decay of DLBS. This may be attributed to the attractiveness of leisure services on a comparatively larger scale and result in smaller distance decay of using DLBS. Education facility density presents a significantly positive relationship with the distance decay coefficient, indicating that AZs with a higher

Table 3
Results of the AGWR model.

Variables	Mean	Std	Min	25%	Median	75%	Max
Population density (PD)	0.0544	0.0256	0.0222	0.0388	0.0454	0.0625	0.0544
Land use entropy (LUE)	0.0166	0.0116	−0.0095	0.0090	0.0153	0.0245	0.0462
Commercial land use ratio (CLUR)	−0.0163	0.0110	−0.0405	−0.0250	−0.0176	−0.0061	0.0017
Public service land use ratio (PSLUR)	−0.0028	0.0137	−0.0419	−0.0124	−0.0005	0.0089	0.0156
Park and square land use ratio (PSQLUR)	−0.0086	0.0145	−0.0389	−0.0220	−0.0082	0.0042	0.0175
Industrial land use ratio (ILUR)	−0.0252	0.0176	−0.0776	−0.0372	−0.0181	−0.0117	−0.0047
Motorway density (MWD)	−0.0147	0.0093	−0.0314	−0.0225	−0.0163	−0.0079	0.0136
Motorized road density (MRD)	0.0013	0.0083	−0.0132	−0.0051	0.0004	0.0062	0.0240
Branch road density (BRD)	0.0139	0.0131	−0.0131	0.0067	0.0133	0.0199	0.0579
Bicycle lane density (BLD)	−0.0108	0.0153	−0.0559	−0.0175	−0.0052	−0.0005	0.0121
Leisure facility density (LFD)	−0.0079	0.0154	−0.0359	−0.0178	−0.0102	−0.0031	0.0384
Education facility density (EFD)	0.0161	0.0118	−0.0009	0.0078	0.0123	0.0229	0.0512
Park and square density (PSQD)	−0.0001	0.0057	−0.0119	−0.0045	−0.0006	0.0037	0.0176
Metro station density (MSD)	0.0127	0.0072	0.0009	0.0070	0.0118	0.0182	0.0311
Bus station density (BSD)	0.0053	0.0137	−0.0263	−0.0055	0.0074	0.0152	0.0304
Parking lot density (PLD)	0.0179	0.0153	−0.0273	0.0117	0.0185	0.0264	0.0490
Number of observations: 620			Akaike's Information Criterion: −1189.888				
R-Squared: 0.662			Adjusted R-Squared: 0.581				

Note: Std denotes standard deviation.

education facility density have larger distance decay of using DLBS. Regrading the factors concerning transit, AZs with more metro stations and parking lots show significantly larger distance decay of using DLBS. Higher transit and private car facilities in an AZ enable the feasibility and convenience to arrive by motorized transport modes, and thus decrease the inclinations of using DLBS for long-distance trips. These may be the underlying reason for the larger distance decay in these areas. The result also shows that AZs with more bus stations tend to have a larger distance decay coefficient, which may be ascribed to the substitution of buses for long-distance trips of using DLBS. However, the effect of bus station density is not significant in statistical tests, probably due to large variations across AZs.

5.3. Variations in the effects of built environments

The above results of MLR are capable of modeling the relationships among built environment factors and the distance decay of using DLBS in a globally spatial perspective. However, we suppose that the distance decay of using DLBS in an AZ is not merely determined by the built environment inside the AZ, but also influenced by the built environment characteristics surrounding the AZ. Simultaneously, we notice that the effects of built environment factors show noticeable variances after calculating the Koenker's Studentized Bruesch-Pagan statistic test (Z-value: 20.376) to examine whether the relationship between distance decay and built environment is consistent across different AZs. Therefore, we further employ the AGWR for analysis, which provides understandings concerning variations in the effects of built environment factors. The results of AGWR are summarized in Table 3, which displays the descriptive statistics of the estimated coefficients for built environment factors in all AZs. The AGWR gives more superior performances in terms of adjusted R^2 (0.581) and Akaike's Information Criterion (-1189.888), as compared to the MLR. The statistics provide general views on the variances in the effects of built environment factors. For instance, the population density has positive influences on the distance decay of DLBS in all AZs, while the bus station density has positive influences on the distance decay of DLBS in more than 50% AZs but negative influences in other AZs. For the sake of visualization, we project the results of AGWR into the AZs and display them in Fig. 6. The red and blue color denotes the built environment factor has positive and negative effects on the distance decay coefficient of using DLBS, respectively. The larger influencing degree is demonstrated by deeper colors. Fig. 6 demonstrates that the effects of each built environment factor on distance decay show variations in geography. The following contents discuss the variances in the influences of each built environment factor and potential underlying reasons.

The population density always presents positive influences on the distance decay of using DLBS, as shown in Fig. 6(a). However, the effect of population density is more pronounced in the southeast part of the study area, which is the newly developed zones in the Pudong district of Shanghai. In these areas, residential communities are commonly built in recent years and matched by business services with clustered characteristics. However, land use intensities of commercial and public services in these areas are low. Residents in these areas may mainly use DLBS for going to destinations around the residential communities (i.e., short-distance trips), but tend to use motorized transport modes for destinations in a farther distance. These may be the potential explanation for the larger effects of population density on the distance decay in these areas.

For the land use characteristics, the effect of land use entropy is positive in most AZs and appears a radial pattern (Fig. 6(b)). The distance decay of DLBS in downtown areas is more affected by land use entropy as compared to AZs farther from the downtown. The difference may be attributed to the higher intensity of land use and convenient transit systems in downtown areas of Shanghai. For the same land use entropy, the AZs in downtown areas have more accessible services in terms of amount and diversity as compared to suburb or rural areas. Therefore, travelers do not need to use DLBS for long-distance trips to reach various life services, and long-distance trips are more likely to be substituted by transit due to the high density of transit facilities in downtown areas. A similar radial pattern can also be observed in the effects of commercial land use ratio. The commercial land use ratio shows larger negative
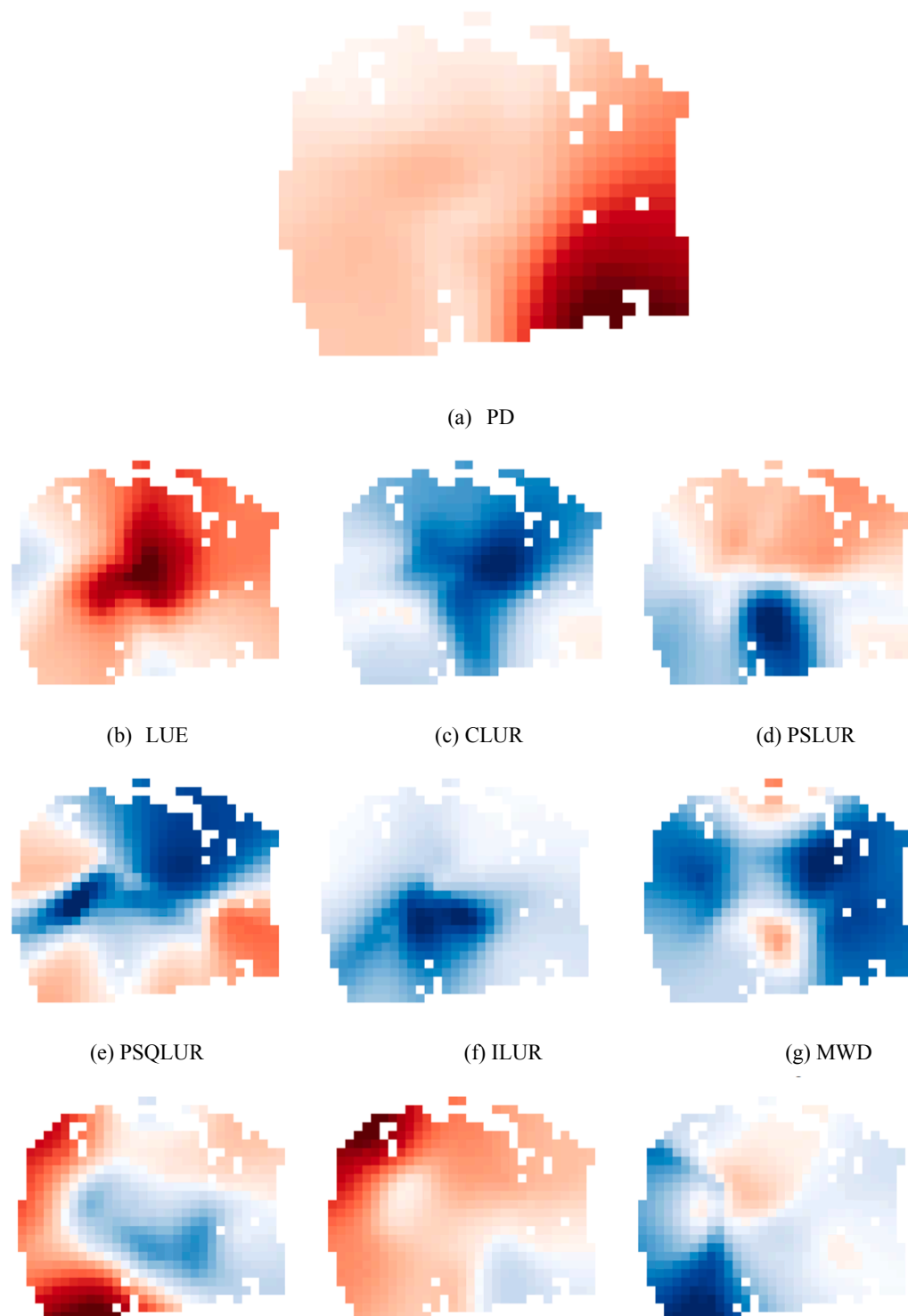
(a) PD

(b) LUE   (c) CLUR   (d) PSLUR

(e) PSQLUR   (f) ILUR   (g) MWD

Fig. 6. Spatial heterogeneity of effects of built environments on distance decay of DLBS.

influences on the distance decay of DLBS in downtown areas (Fig. 6(c)). The potential reason may be that higher commercial ratios in central areas produce stronger siphonage to attract or disperse people from or to a larger scale. These may attract more long-distance trips of using DLBS from and to these areas. Moreover, the commercial areas in downtown are commonly short of available parking lots
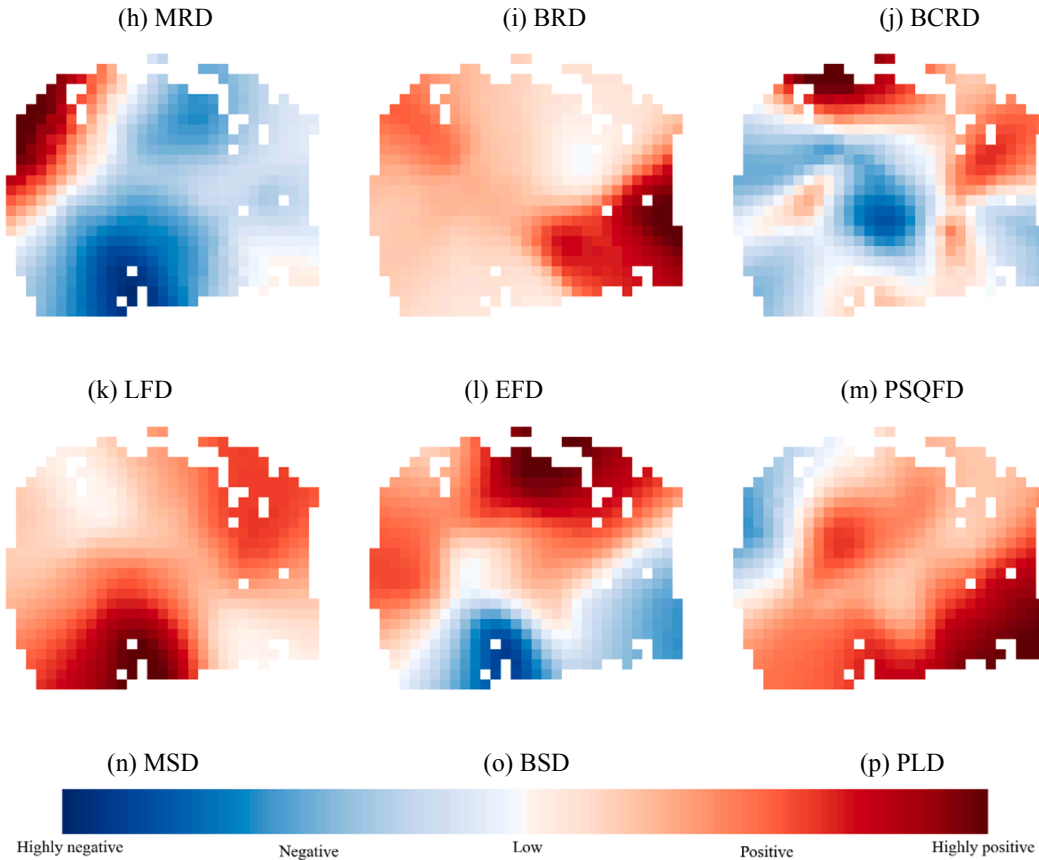
Fig. 6. (*continued*).

and have more severe traffic congestions, which encourages usage of DLBS for longer trips instead of motorized transport modes. Fig. 6 (d) shows that the public service land use ratio has positive influences on the distance decay of DLBS in the north part of the study area containing the northern parts of Yangpu, Baoshan and Pudong districts, which are mostly suburban or rural areas. Public services in these areas mainly serve local communities and do not attract residents far from the locations. In contrast, the public service land use ratio shows a negative influence in some areas including Xuhui, Changning, and south part of Pudong districts. There are a lot of global public services in these areas for all residents in Shanghai (e.g., hospitals, vehicle management departments, and schools), which would attract or radiate people from or to farther places by using DLBS. This may be a potential explanation for the negative influence of public service land use ratio on the distance decay in these areas. The park and square land use ratio has negative influences on the distance decay of DLBS in most AZs (Fig. 6(e)), but show positive influences in the southeast, northwest and southwest corners of the study area. The difference may be ascribed to the distinctions in transit facilities to parks or squares and service areas. For example, if parks and squares have convenient metro and bus stations nearby, or mainly attract local residents around the parks/squares rather than residents from other areas, most usages of DLBS in such areas tend to be short-distance trips (namely larger distance decay). The industrial land use ratio shows negative influences on the distance decay of DLBS in all AZs (see Fig. 6(f)), and is more notable in the areas of Jingan, Huangpu, west part of Pudong and north part of Xuhui district where traffic congestions are severe in peak hours and parking lots are not sufficient. These may encourage travelers in these areas to use DLBS for long-distance trips instead of motorized transport modes.

With regards to the built environment factors concerning design, the motorway density has negative influences on the distance decay of DLBS in most AZs (Fig. 6(g)), but show smaller impacts in some areas such as Huangpu and Xuhui districts. The negative influence of motorway density may be explained by the fact that the motorways in Shanghai are not allowed for bikes, as discussed in Section 5.2. However, some areas have high densities of both motorway and branch road, so the connectivity by DLBS is not severely reduced by motorways in these areas, which might be the reason for the observed differences. In most AZs, the branch road density shows positive effects on the distance decay (Fig. 6(i)), except the southeast part of the study area (i.e., the aforementioned new development area in Pudong district with dispersed land use characteristics). Higher branch road density in such areas with dispersed services may encourage travelers to use DLBS for comparatively longer trips for reaching various services, namely smaller distance decay as compared to others. The effect of motorized road density (including primary and secondary roads) presents large spatial variations (Fig. 6(h)), which may be attributed to the differences in cross-sectional forms of motorized roads in different areas. Cross-

sectional forms of primary and secondary roads in different areas of Shanghai are very distinct in terms of lane settings. The AZs with positive influences mainly distribute in the west parts of Xuhui, Baoshan, Changning, and Putuo districts. Most primary and secondary roads in these areas have mixed traffic flow with high traffic volumes of motorized vehicles and terrible road environments for bicycling due to lack of convenient side lanes. These would discourage the accessibility, safety and usage of DLBS for destinations with long distances. Combining with the effect of bike-dedicated lanes in Fig. 5(j), we can observe that higher bike lane density in the similar areas can reduce the distance decay of DLBS more pronounced than other areas, which may be ascribed to the fact that dedicated lanes for bike improve the road environment for bicycling in primary and secondary roads of these areas and thus enhance the usage of DLBS to farther places. In contrast, the primary and secondary roads in other AZs have side lanes and thus are comparatively friendly for bicycling. Therefore, higher primary and second road densities in these areas could slightly reduce the distance decay of DLBS, and more bike-dedicated lanes do not have substantial effects on the distance decay of DLBS, as can be observed from Fig. 6(h) and (j).

As for factors about destinations, the leisure facility density (Fig. 6(k)) has negative effects on the distance decay of DLBS in most AZs, but positive effects in the northwest part of the study areas, including the west parts of Putuo and Baoshan districts. The potential explanation for the positive effects in some AZs could be that the leisure facilities in those areas are targeted at serving local communities, rather than for residents on a large scale. In all AZs, the education facility density (Fig. 6(l)) shows positive influences that are more notable in the new development area of the Pudong district. Fig. 6 (m) demonstrates a dispersed effect of park and square density on the distance decay of DLBS, which is similar to the results about the park and square ratio land use.

Regarding built environment factors about the distance to transit, Fig. 6(n) shows that the metro station density has positive influences on the distance decay of DLBS, which is logical as higher metro station density means long-distance trips of DLBS are more likely to be substituted by metro. The influence is more pronounced in the east part of Xuhui district and south part of Pudong district, which may be ascribed to the metro-oriented-developed patterns in these areas. Residents and services are concentrated around metro stations, which may lead to more short-distance trips in such areas. For the effect of bus station density, it shows positive influences in most AZs as the bus is a competitor of DLBS for comparatively long trips. However, we do not anticipate that the bus station density decreases the distance decay of DLBS in some AZs, as shown in Fig. 5(o). This counterintuitive phenomenon needs further explorations based on other data. The effect of parking lot density on the distance decay of DLBS is positive in almost all AZs and more remarkable in the new development area of the south of Pudong district (Fig. 6(p)). As mentioned before, the new development areas in the southeast of Pudong district have clustered land use characteristics and less dense commercial services. More parking lots would provide more convenience for using the private car to various places, and reduce the likeliness of using DLBS for long trips.

In short, the results of AGWR indeed reveal that the influences of built environment factors on the distance decay of DLBS have apparent heterogeneities in different urban areas. We can observe the distinct effects of a built environment factor among downtown, suburban, and new development areas. The law of distance decay of human movements, herein the movements by DLBS, is affected by many factors including infrastructure, land use, and the demographic attributes of residents. These influencing factors may have coupling effects to some extent, which may be the underlying reasons for the observed spatial heterogeneity in the effects of built environment factors.

6. Conclusions and implications

As an environmentally friendly alternative to traditional travel modes and promising sharing economics, the micro-sharing mobility systems such as DLBS are being embraced by metropolises around the world. However, their performances, usage patterns, and interactions with the built environments are insufficiently investigated for effective planning and management of these systems. This study endeavors to fill up the gaps in relevant research by deciphering the spatial heterogeneity of the distance decay of using DLBS and their relationships with the built environment based on empirical analysis in Shanghai of China. These are targeted at comprehensive understandings concerning the spatial interactions by DLBS to support sustainable planning and promotion of DLBS in various urban contexts. The main contributions and findings of this study can be summarized as follows.

We extract the trip distance distributions of using DLBS in different contexts of a city combining large-scale transaction data of DLBS and online routing API. Particularly, we utilize online routing API to acquire the plausible riding routes and distances based on the transaction records, rather than using Euclidean distance. The distance decay functions in different areas are empirically estimated based on AZ-based datasets. We find notable spatial heterogeneity in the distance decay of using DLBS in different urban contexts. The distance decay of using DLBS is discussed from statistical and spatial perspectives.

Leveraging multi-source data, we obtain various built environment factors concerning density, diversity, design, destination, and distance to transit in different urban areas. A term frequency-inverse document frequency model is proposed to extract land use characteristics based on POI data and to amend the imbalance features of online POI data. MLR is used to model the associations of built environment factors with the distance decay of using DLBS in a global view for explaining spatial heterogeneity of distance decay. Results indicate that several built environments indeed have significant effects on the law of distance decay for DLBS. Built environment factors including population density, education facility density, land use entropy, branch road density, metro station density, and parking lot density are positively related to distance decay of using DLBS, indicating areas with higher degrees of these factors have faster distance decay of using DLBS. In contrast, commercial land use ratio, industrial land use ratio and park and square land use ratio, motorway density, and leisure facility density are found to be negatively associated with the distance decay of using DLBS. Importantly, we find that the effects of some factors (e.g., population density) on the distance decay of DLBS differ from their effects on the distance decay of motorized transport modes.

Lastly, AGWR is employed to further investigate the spatial variations of the influences of built environment factors on the distance decay of using DLBS. Results demonstrate notable variations exist in the influences of built environment factors and some factors such

Table A.1

POI categories from Amap and corresponding land use categories.

Land use categories	Code	POI category	Land use categories	Code	POI category
Living land use	1	Residential buildings and areas	Commercial service	23	Cafe/Tea shops
Public management and service land use	2	Post office	land use	24	Leisure food shops
	3	Municipal water supply service department		25	Shopping mall
	4	Municipal electricity supply service department		26	Convenience mini-stores
	5	Hospital		27	Electronic products stores
	6	Pharmacy		28	Supermarkets
	7	Judiciary and police authorities		29	Plants and pet markets
	8	Governmental organizations and social communities		30	Furniture and building materials markets
	9	Museum		31	Sport/Stationary shops
	10	Exhibition hall		32	Clothing stores
	11	Library		33	Telecom stores/office
	12	Public media organization		34	Beauty and hairdressing service
	13	School and education institutions		35	Electronics repair and service
Road and transport infrastructure land use	14	Transport service and facilities		36	Baby product and service
Park and square land use	15	Park/square		37	Sports Stadium
Industrial land use	16	Factories and planting base		38	Recreation stores and center
Commercial service land use	17	Car Sales		39	Theatre/cinema
	18	Car repair service		40	Hotel
	19	Motorcycle service		41	Tourism spots
	20	Chinese restaurant		42	Bank and ATM
	21	Foreign restaurant		43	Insurance company
	22	Fast food restaurant		44	Company and business

as dedicated bike lanes, public service land use ratio, and motorized road density present opposite effects on the distance decay of using DLBS in different contexts. The results imply the necessity of considering the divergent effect of the built environment in geography. Comprehensive discussions are conducted to provide empirical explanations concerning the varying effects of built environment factors. The AGWR offers more accurate modeling towards the law of distance decay using DLBS in a microscope perspective.

The above findings provide practical implications for the management and planning of DLBS. The spatial heterogeneity in the distance decay of using DLBS suggests that it is implausible to apply a spatially homogeneous distance decay function to predict the intensity of spatial interactions by DLBS. In forecasting the spatial demand for DLBS, it is necessary to develop customized models based on the specific characteristics in different urban space in case of biases, which has been attached little attention in the literature. Moreover, the results in MLR and AGWR decipher the variations in the distance decay of using DLBS from a geographical perspective. The obtained quantitative results such as the effects of different built environment factors, could be scientific supports and referential values for demand predictions of DLBS, especially for areas that the DLBS does not exist yet or is in its early stage. For instance, the calibrated MLR and AGWR can be utilized to predict the distance decay functions of different areas based on their known built environment statistics, and be utilized in the famous land use and transport model (e.g., Gravity Model). This would serve the accurate demand forecasting and thus supply allocations of DLBS, which would be useful for achieving supply–demand balances of DLBS in different urban areas. These are also great practical supports for the DLBS companies to allocate and rebalance the bikes to fulfill the usage demand of DLBS, and thus realize a high utilization rate of every shared bike. This is particularly crucial for bike-sharing startup companies that have limited bikes in the early stage and need to improve utilization rates of a bike for reducing budgets. Simultaneously, the distance decay is a useful reference for the bike-sharing companies to determine pricing strategies (i.e., the relationship between riding distance/time with prices). For instance, most users only use DLBS for short-distance trips; some discounts can be given for relatively long trips to attract more users and increase ridership of DLBS and the pricing rule could be determined based on the distance decay function in an area (e.g., the riding distance threshold of providing discounts). Moreover, insights into the effects of built environment factors such as land use and transport infrastructure, offer empirical and quantitative instruments for evaluating the accessibility of using DLBS to various services in different urban contexts. These produce implications and directions for the land use and infrastructure planning that is aimed to promote the usage of DLBS. For example, the results indicate that increasing the commercial land use ratio could attract users to use DLBS for comparatively longer trips. Therefore, a DLBS could be matched with new commercial areas to be developed in the early planning stage for inducing nearby residents to use sharing bikes to reach the commercial areas and forming the traveling habits of use DLBS in the future. These further add values to enhancing the mutually reinforcing developments of land use and DLBS to establish an environmentally friendly transport system and sustainable urban communities.

However, this study has several aspects that could be further extended. Firstly, our datasets do not include information about trip purposes. The distance decay of using DLBS for different purposes may be different and show spatial variations in urban space. Secondly, we do not consider the socioeconomic characteristics in different areas due to data limitations. Nonetheless, it is anticipated that socioeconomic characteristics such as income, age, and gender may influence the law of distance decay. Besides, it is also interesting to examine the potential nonlinear and interaction effects of different built environment factors on the distance decay of

using DLBS, which has the potentials to further explain the varying influences of different factors. Moreover, our empirical analysis merely analyzed the DLBS in Shanghai of China. How the travelers use the DLBS for trips of different distances is expected to be related to the urban contexts and user behavior (e.g., using bikes for commuting is very prevalent in the Netherlands even the trip distance is long). It is interesting to compare the distance decay of using DLBS in different cities with different urban contexts and user behaviors, especially in different nations. Lastly but not at least, some calculation methods regarding built environment factors could be further improved. For instance, the used entropy method to calculate land use mix feature has limitations in terms of considering the layout of different types of land use and the scale of each zone (Guo et al., 2016, 2017; Song et al., 2013). More advanced methods for quantifying the built environment factors (Lang et al., 2018; Sarkar and Chunchu, 2016) could be incorporated in future work for addressing these limitations.

CRediT authorship contribution statement

Kun Gao: Methodology, Formal analysis, Writing - original draft. **Ying Yang:** Conceptualization, Methodology, Resources, Supervision, Writing - review & editing. **Aoyong Li:** . **Xiaobo Qu:** Resources, Supervision, Writing - review & editing.

Acknowledgment

Thanks for the Amap company provide us the developer ports to use routing and POI API, which offer us the data for our analysis. We would like to express our appreciations to the reviewers for providing valuable suggestions regarding improving the paper quality.

Declaration of Competing Interest

On behalf of all authors, the corresponding author states that there is no conflict of interest.

Appendix A

See Table A.1.

References

Arranz-López, A., Soria-Lara, J.A., Witlox, F., Paez, A., 2019. Measuring relative non-motorized accessibility to retail activities. Int. J. Sustainable Transport. 13 (9), 639–651.
Bao, J., Xu, C., Liu, P., Wang, W., 2017. Exploring bikesharing travel patterns and trip purposes using smart card data and online point of interests. Networks Spatial Econ. 17 (4), 1231–1253.
Barbour, N., Zhang, Y., Mannering, F., 2019. A statistical analysis of bike sharing usage and its potential as an auto-trip substitute. J. Transport Health 12, 253–262.
Brunsdon, C., Fotheringham, A.S., Charlton, M.E., 1996. Geographically weighted regression: a method for exploring spatial nonstationarity. Geograph. Anal. 28 (4), 281–298.
Cervero, R., 1988. Land Use Mixing and Suburban Mobility. Transport. Quart. 42, 429–446.
Cervero, R., Kockelman, K., 1997. Travel demand and the 3Ds: Density, diversity, and design. Transport. Res. Part D, Transport Environ. 2 (3), 199–219.
Cervero, R., Sarmiento, O.L., Jacoby, E., Gomez, L.F., Neiman, A., 2009. Influences of built environments on walking and cycling: lessons from Bogotá. Int. J. Sustainable Transport. 3 (4), 203–226.
Chen, Z., van Lierop, D., Ettema, D., 2020. Dockless bike-sharing systems: what are the implications? Transport Rev. 1–21.
De Vries, J.J., Nijkamp, P., Rietveld, P., 2009. Exponential or power distance-decay for commuting? An alternative specification. Environ. Plann. A 41 (2), 461–480.
El-Assi, W., Mahmoud, M.S., Habib, K.N., 2017. Effects of built environment and weather on bike sharing demand: a station level analysis of commercial bike sharing in Toronto. Transportation 44 (3), 589–613.
Fotheringham, A.S., O'Kelly, M.E., 1989. Spatial Interaction Models: Formulations and Applications. Kluwer Academic Publishers Dordrecht.
Gao, K., Yang, Y., Li, A., Li, J., Yu, B., 2021. Quantifying economic benefits from free-floating bike-sharing systems: A trip-level inference approach and city-scale analysis. Transport. Res. Part A: Policy Pract. 144, 89–103.
Gao, K., Yang, Y., Sun, L., Qu, X., 2020. Revealing psychological inertia in mode shift behavior and its quantitative influences on commuting trips. Transport. Res. Part F: Traff. Psychol. Behav. 71, 272–287.
Gao, K., Yang, Y., Zhang, T., Li, A., Qu, X., 2021. Extrapolation-enhanced model for travel decision making: An ensemble machine learning approach considering behavioral theory. Knowl.-Based Syst. 218, 106882.
Guo, Y., Agrawal, S., Peeta, S., Somenahalli, S., 2016. Impacts of property accessibility and neighborhood built environment on single-unit and multiunit residential property values. Transp. Res. Rec. 2568 (1), 103–112.
Guo, Y., He, S.Y., 2020. Built environment effects on the integration of dockless bike-sharing and the metro. Transport. Research Part D: Transport Environ. 83, 102335.
Guo, Y., Peeta, S., Somenahalli, S., 2017. The impact of walkable environment on single-family residential property values. J. Transport Land Use 10 (1), 241–261.
Hakim, A.A., Erwin, A., Eng, K.I., Galinium, M., Muliady, W., 2014. Automated document classification for news article in Bahasa Indonesia based on term frequency inverse document frequency (TF-IDF) approach. 2014 6th International Conference on Information Technology and Electrical Engineering (ICITEE). IEEE.
Halás, M., Klapka, P., Kladivo, P., 2014. Distance-decay functions for daily travel-to-work flows. J. Transp. Geogr. 35, 107–119.
Han, S.Y., Tsou, M.-H., Clarke, K.C., 2018. Revisiting the death of geography in the era of Big Data: the friction of distance in cyberspace and real space. Int. J. Digital Earth 11 (5), 451–469.
Hipp, J.R., Boessen, A., 2017. The shape of mobility: Measuring the distance decay function of household mobility. Profess. Geographer 69 (1), 32–44.
Hua, M., Chen, X., Zheng, S., Cheng, L., Chen, J., 2020. Estimating the parking demand of free-floating bike sharing: A journey-data-based study of Nanjing, China. J. Cleaner Prod. 244, 118764.
Iacono, M., Krizek, K., El-Geneidy, A.M., 2008. Access to Destinations: How Close is Close Enough? Estimating accurate Distance decay Functions for Multiple Modes and Different Purposes. Minnesota Department of Transportation, St. Paul, MN.

Ji, Y., Jin, X., Ma, X., Zhang, S., 2020. How does dockless bike-sharing system behave by incentivizing users to participate in rebalancing? IEEE Access 8, 58889–58897.

Jin, S., Qu, X., Zhou, D., Xu, C., Ma, D., Wang, D., 2015. Estimating cycleway capacity and bicycle equivalent unit for electric bicycles. Transport. Res. Part A: Policy Pract. 77, 225–248.

Kang, C., Sobolevsky, S., Liu, Y., Ratti, C., 2013. Exploring human movements in Singapore: a comparative analysis based on mobile phone and taxicab usages. In: Proceedings of the 2nd ACM SIGKDD International Workshop on Urban Computing, pp. 1–8.

Kong, X., Liu, Y., Wang, Y., Tong, D., Zhang, J., 2017. Investigating public facility characteristics from a spatial interaction perspective: A case study of Beijing hospitals using taxi data. ISPRS Int. J. Geo-Inf. 6 (2), 38.

Kou, Z., Cai, H., 2019. Understanding bike sharing travel patterns: An analysis of trip data from eight cities. Physica A 515, 785–797.

Krizek, K.J., El-Geneidy, A., Thompson, K., 2007. A detailed analysis of how an urban trail system affects cyclists travel. Transportation 34 (5), 611–624.

Lang, W., Long, Y., Chen, T., 2018. Rediscovering Chinese cities through the lens of land-use patterns. Land Use Policy 79, 362–374.

Lazarus, J., Pourquier, J.C., Feng, F., Hammel, H., Shaheen, S., 2020. Micromobility evolution and expansion: Understanding how docked and dockless bikesharing models complement and compete–A case study of San Francisco. J. Transp. Geogr. 84, 102620.

Li, A., Huang, Y., Axhausen, K.W., 2020. An approach to imputing destination activities for inclusion in measures of bicycle accessibility. J. Transp. Geogr. 82, 102566.

Lin, L., Li, W., Peeta, S., 2020 Predicting Station-Level Bike-Sharing Demands Using Graph Convolutional Neural Network, arXiv preprint arXiv:2004.08723.

Liu, H.-C., Lin, J.-J., 2019. Associations of built environments with spatiotemporal patterns of public bicycle use. J. Transp. Geogr. 74, 299–312.

Lovelace, R., Goodman, A., Aldred, R., Berkoff, N., Abbas, A., Woodcock, J., 2017. The Propensity to Cycle Tool: An open source online system for sustainable transport planning. J. Transport Land Use 10 (1), 505–528.

Martínez, L.M., Viegas, J.M., 2013. A new approach to modelling distance-decay functions for accessibility assessment in transport studies. J. Transp. Geogr. 26, 87–96.

Mateo-Babiano, I., Bean, R., Corcoran, J., Pojani, D., 2016. How does our natural and built environment affect the use of bicycle sharing? Transport. Rese. Part A: Policy Practice 94, 295–307.

Pal, A., Zhang, Y., 2017. Free-floating bike sharing: Solving real-life large-scale static rebalancing problems. Transport. Res. Part C: Emerg. Technol. 80, 92–116.

Sarkar, P.P., Chunchu, M., 2016. Quantification and analysis of land-use effects on travel behavior in smaller Indian cities: case study of Agartala. J. Urban Plann. Dev. 142 (4), 04016009.

Shui, C.S., Szeto, W., 2018. Dynamic green bike repositioning problem–A hybrid rolling horizon artificial bee colony algorithm approach. Transport. Res Part D: Transport Environ. 60, 119–136.

Siła-Nowicka, K., Fotheringham, A.S., 2019. Calibrating spatial interaction models from GPS tracking data: an example of retail behaviour. Comput. Environ. Urban Syst. 74, 136–150.

Song, Y., Merlin, L., Rodriguez, D., 2013. Comparing measures of urban land use mix. Comput. Environ. Urban Syst. 42, 1–13.

Sun, Y., Mobasheri, A., Hu, X., Wang, W., 2017. Investigating impacts of environmental factors on the cycling behavior of bicycle-sharing users. Sustainability 9 (6), 1060.

Sun, Z., Wang, Y., Zhou, H., Jiao, J., Overstreet, R.E., 2019. Travel behaviours, user characteristics, and social-economic impacts of shared transportation: a comprehensive review. Int. J. Logistics Res. Appl. 1–28.

Svegander, M., 2020. The Bike and Scooter- sharing Telematics Market. Stockholm, Sweden.

Tobler, W.R., 1970. A computer movie simulating urban growth in the Detroit region. Econ. Geography 46, 234–240.

Van Wee, B., 2002. Land use and transport: research and policy challenges. J. Transp. Geogr. 10 (4), 259–271.

Wang, Y., Douglas, M.A., Hazen, B.T., Dresner, M., 2018. Be green and clearly be seen: How consumer values and attitudes affect adoption of bicycle sharing. Transport. Res. Part F: Traffic Psychol. Behav. 58, 730–742.

Wang, Y., Jia, S., Zhou, H., Charlton, S., Hazen, B., 2020. Factors affecting orderly parking of dockless shared bicycles: an exploratory study. Int. J. Logist. Res. Appl. 1–23.

Wang, Y., Yang, Y., Wang, J., Douglas, M., Su, D., 2021. Examining the influence of social norms on orderly parking behavior of dockless bike-sharing users. Transport. Res. Part A: Policy Pract. 147, 284–296.

Yang, X., Fang, Z., Xu, Y., Yin, L., Li, J., Lu, S., 2019. Spatial heterogeneity in spatial interaction of human movements—Insights from large-scale mobile positioning data. J. Transp. Geogr. 78, 29–40.

Yasmin, F., Larsen, J., El-Geneidy, A., 2010. Examining travel distances by walking and cycling, Montréal, Canada. 89th Annual Meeting of the Transportation Research Board, Washington, DC.

Yin, L., Wang, Q., Shaw, S.-L., Fang, Z., Hu, J., Tao, Y., Wang, W., 2015. Re-identification risk versus data utility for aggregated mobility research using mobile phone location data. PLoS One 10 (10), e0140589.

Zhang, M., Zhao, P., 2017. The impact of land-use mix on residents travel energy consumption: New evidence from Beijing. Transport. Res. Part D: Transport Environ. 57, 224–236.

Zhang, Y., Mi, Z., 2018. Environmental benefits of bike sharing: A big data-based analysis. Appl. Energy 220, 296–301.

Zhang, Y., Thomas, T., Brussel, M., Van Maarseveen, M., 2017. Exploring the impact of built environment factors on the use of public bikes at bike stations: case study in Zhongshan, China. J. Transport Geography 58, 59–70.

Zhou, S., Lin, R., 2019. Spatial-temporal heterogeneity of air pollution: The relationship between built environment and on-road PM2. 5 at micro scale. Transport. Res. Part D: Transport Environ. 76, 305–322.

Zhu, Y.-J., Hu, Y., Collins, J.M., 2020. Estimating road network accessibility during a hurricane evacuation: A case study of hurricane Irma in Florida. In: Transport. Res. Part D: Transport Environ., p. 102334.